Collating Airborne and Surface Observations of the Microstructure of Precipitating Continental Convective Clouds

J. DOYNE SARTOR AND THEODORE W. CANNON

National Center for Atmospheric Research,[1] Boulder, Colo. 80307

(Manuscript received 8 December 1975, in revised form 9 May 1977)

ABSTRACT

The observational results from sailplane flights into the updrafts of developing cumulus clouds in northeastern Colorado show some important variations in the microstructure of the cloud droplet and ice particle distributions. Some of these variations are apparently caused by the combined interactions of cloud droplets and precipitation particles with the horizontal and vertical components of the updraft and its horizontal and vertical structure.

Data from these observations are introduced into a circulation framework in an attempt to understand how the microphysics and the circulation can interact to give the features observed. The results cast doubt on the validity of the often made assumption that the microphysical properties of a cloud are distributed randomly with respect to each other on the smaller scales, and that this condition exists uniformly throughout the cloud.

The observed precipitation shafts with bimodal size distributions in the middle and lower parts of a cloud can be recreated in a two-dimensional simulation of the observed cloud air circulation with embedded microphysics. The observed and calculated frozen water content can increase by one to two orders of magnitude over the liquid water content when moving from cloudy air into a precipitation shaft. The observed change in concentration with height of the ice particles exceeds (by over two orders of magnitude) the expected ice nuclei concentration usually found in the atmosphere at comparable temperatures. The average concentrations of ice particles observed occasionally exceed 400 ℓ^{-1}.

1. Introduction

The observational results from sailplane flights into the updrafts of developing cumulus clouds in northeastern Colorado show some important variations in the microstructure of the cloud droplet and ice particle distributions. Some of these variations are apparently caused by the combined interactions of cloud droplets and precipitation particles with the horizontal and vertical components of the updraft and its horizontal and vertical structure.

The time and space resolution of the sailplane measurements were chosen to be as small as possible so that the planned observations could be used to evaluate one of the fundamental assumptions of most cloud models, i.e., that the microphysical properties of a cloud are located randomly with respect to each other but are distributed uniformly over the larger scales. These requirements could be met more easily with the sailplane due to its ability to ascend close to updraft velocity and its much lower forward air speed than than of a conventional aircraft. Some of the results of these observations are introduced into a single-cell circulation framework in an attempt to determine whether or not the microphysics and the circulation can interact to give the anomalies observed.

2. Methods of observations and instrumentation

The observations were taken with instruments installed on the NOAA-NCAR sailplane *Explorer*. Usually the sailplane was towed into the updraft of a growing cumulus cloud and released to be carried up into the cloud by the rising motion of the air. The sailplane circles as closely as possible to the core of the updraft so that the measurements are made in a clearly identifiable motion field in the cloud that will contain the most crucial microphysical processes leading directly to the production of precipitation. A similar technique of flying in the updraft and obtaining microphysical information using a small, powered aircraft in a seeded cumulus cloud near Flagstaff, Ariz., has been described by Todd (1965).

The instrumentation on the sailplane at the time of the observations described here is given in Table 1. Sartor (1972) and Sartor and Toutenhoofd (1973) contain more detailed descriptions of the sailplane and its instrumentation.

[1] This research was performed as part of the National Hail Research Experiment, managed by the National Center for Atmospheric Research and sponsored by the Weather Modification Program, Research Applications Directorate, National Science Foundation.

TABLE 1. 1972 instrumentation of the *Explorer* sailplane.

Instrument	Range*	Accuracy	Sampling volume* and/or time resolution
Camera: *in situ* particles, liquid and solid	For concentrations, ≥ 4 μm; for sizing, ≥ 8 μm	$\pm 20\%$	5 cm^3 for 10 μm droplets, 50 cm^3 for 0.5 mm ice; 0.5 s
Electrostatic cloud droplet disdrometer	4–13 μm in 1.5 μm intervals, 13–19 μm in 3 μm intervals and 19–100 μm in one interval	$\pm 10\%$	1.0 cm^3 per 0.5 s to 13 μm; >13 μm, 8 cm^3 per 4 s sample
Cloud droplet impactor slides	≥ 2 μm	$\pm 15\%$	50 cm^3, occasional sample
Variometer, vertical speed of sailplane	-40 to $+40$ m s^{-1}	± 0.4 m s^{-1}	<0.5 s
Pressure altitude	1010 120 mb	± 0.5 mb	<1 s (0.5 mb pressure)
Temperature	-75 to $+30$°C	Unknown	To be determined after computerized analysis
Indicated airspeed	0–67 m s^{-1}	± 4 m s^{-1}	<0.5 s
Vertical accelerometer	$-10g$ to $+10g$	$\pm 0.3g$	<0.5 s
Lyman-alpha humidiometer	-40 to $+20$°C	± 2°C	<0.1 s

* Particle-size dimensions are radii.

Cloud droplet distributions were obtained automatically with an instrument (Abbott *et al.*, 1972) that responds electrostatically to the size of the impinging droplets and counts the number in each of nine channels according to the format listed in Table 1.

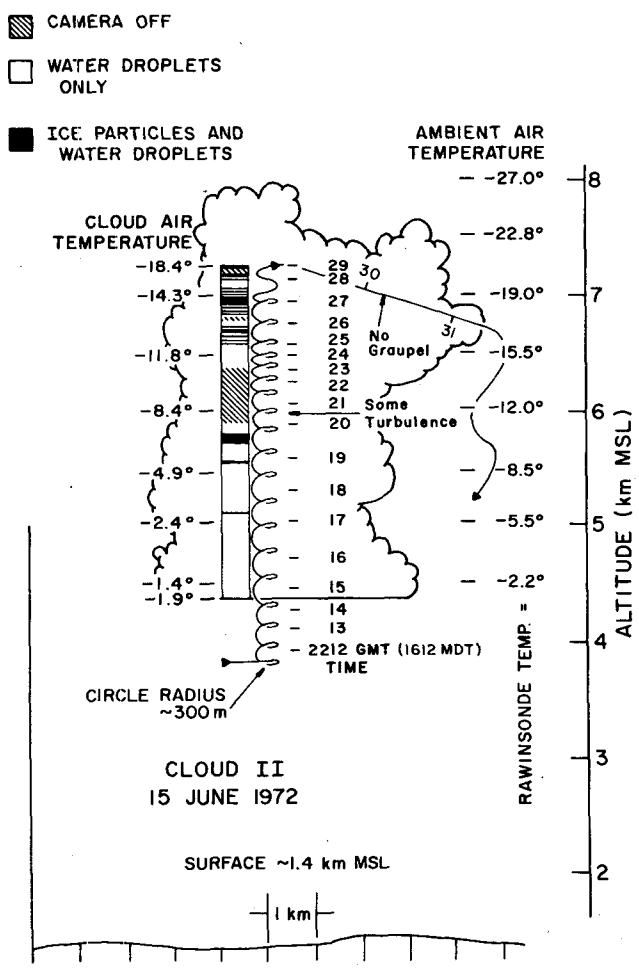

FIG. 1. Schematic drawing of a portion of the flight of 15 June 1972.

A special camera system (Cannon, 1974) was used to determine the size and concentration of ice particles and water drops, and to distinguish between ice and water when the particles are 100 μm diameter or larger. The comparison of the data from the two instruments, the Cannon camera for ice particle and water drop populations and the electrostatic disdrometer for automatic cloud droplet distributions, gives an extra degree of confidence in the measurements and provides recognition of certain questionable data—an invaluable aid in these studies.

3. Observational detail

The flights were made with the sailplane into cumulus clouds in connection with the National Hail Research Experiment (NHRE) in northeastern Colorado, during the summer months of 1971 and 1972. The clouds varied from a few hundred meters depth to rapidly developing precipitating cumuli of several thousand meters vertical thickness; and from isolated cells to new growth appendages of fully developed thunderstorms. The microphysics, the updrafts and the meteorological environments of two contrasting clouds, one on 15 June 1972 and the other on 23 June 1972, are used to examine the physical processes in these two widely different situations. Both days were NHRE seed days, but the measured hail output in the NHRE protected area on 23 June was over an order of magnitude greater than on 15 June.

a. 15 June 1972

A schematic drawing of the flight made in the updraft of a developing cumulus cloud on 15 June 1972 in northeastern Colorado is shown in Fig. 1. The flight path is projected onto a vertical plane and is drawn

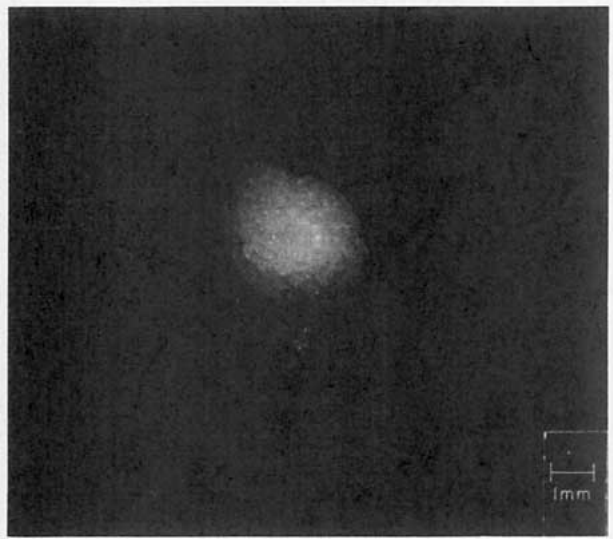

FIG. 2. Melting graupel particle photographed on 15 June 1973 at 3.1 km MSL, $T=6.2°C$, in precipitation from cumulus cloud.

roughly to scale including the size and spacings of the loops traced by the sailplane as it spiraled upward in the updraft. Except for the altitude of cloud base and the dimensions of the cloud from the apogee of the sailplane flight to the cloud edge, the form and dimensions of the cloud are largely fiction. The portions of the flight path where *water droplets only* appeared and where *ice and water droplets* occurred together, as determined from the *in situ* photographs at 0.5 s intervals, are indicated in the diagram of Fig. 1 according to whether the vertical bar graph is unmarked or is solid black (often appearing as thin horizontal lines because of very short intervals when ice particles appear).

The ice particles seldom exhibit a crystalline or spherical shape but are usually irregular or amorphous in form, suggesting growth by the accretion of supercooled cloud droplets. Close-up photographs similar to that of Fig. 2, taken in a precipitation shaft of a developing cumulus cloud on 15 June 1973, add weight to the evidence that the ice particles were formed largely by accretion. A large number of these ice particles have been captured in similar clouds and studied by Knight *et al.* (1974), confirming the preponderance of graupel in the early stages of precipitation growth in these clouds.

The microphysical detail of the observations is illustrated with data from the minute 1619 MDT (2219 GMT) of the flight on 15 June 1972 in Fig. 3. Starting at the top of Fig. 3 the computerized output plots show the vertical speed of the air, the liquid water content (LWC), the total cloud droplet concentration (labeled T), and the cloud particle size and concentration distributions (labeled 5, 6, 8, 9 and 11) as functions of time. The measurements illustrated in Fig. 3 are fairly

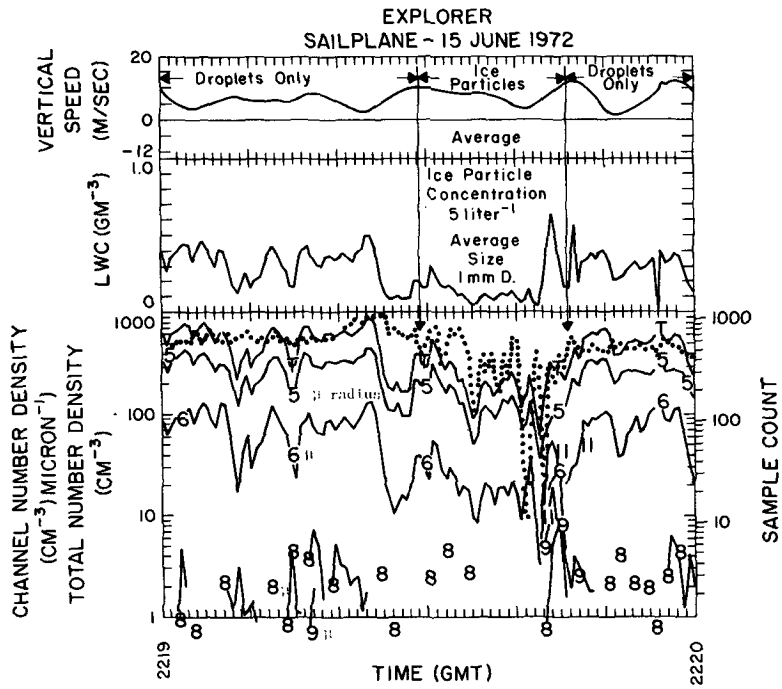

FIG. 3. Vertical airspeed, liquid water content and droplet concentration from electrostatic disdrometer and particle camera for the minute 2219 GMT on 15 June 1972. The solid lines numbered 5, 6, 8, 9 and 11 refer to the characteristic radius (μm) of the cloud droplets; the total number density (cm^{-3}) is shown by the line marked T. Droplet concentration from the particle camera photographs is plotted as the dotted line.

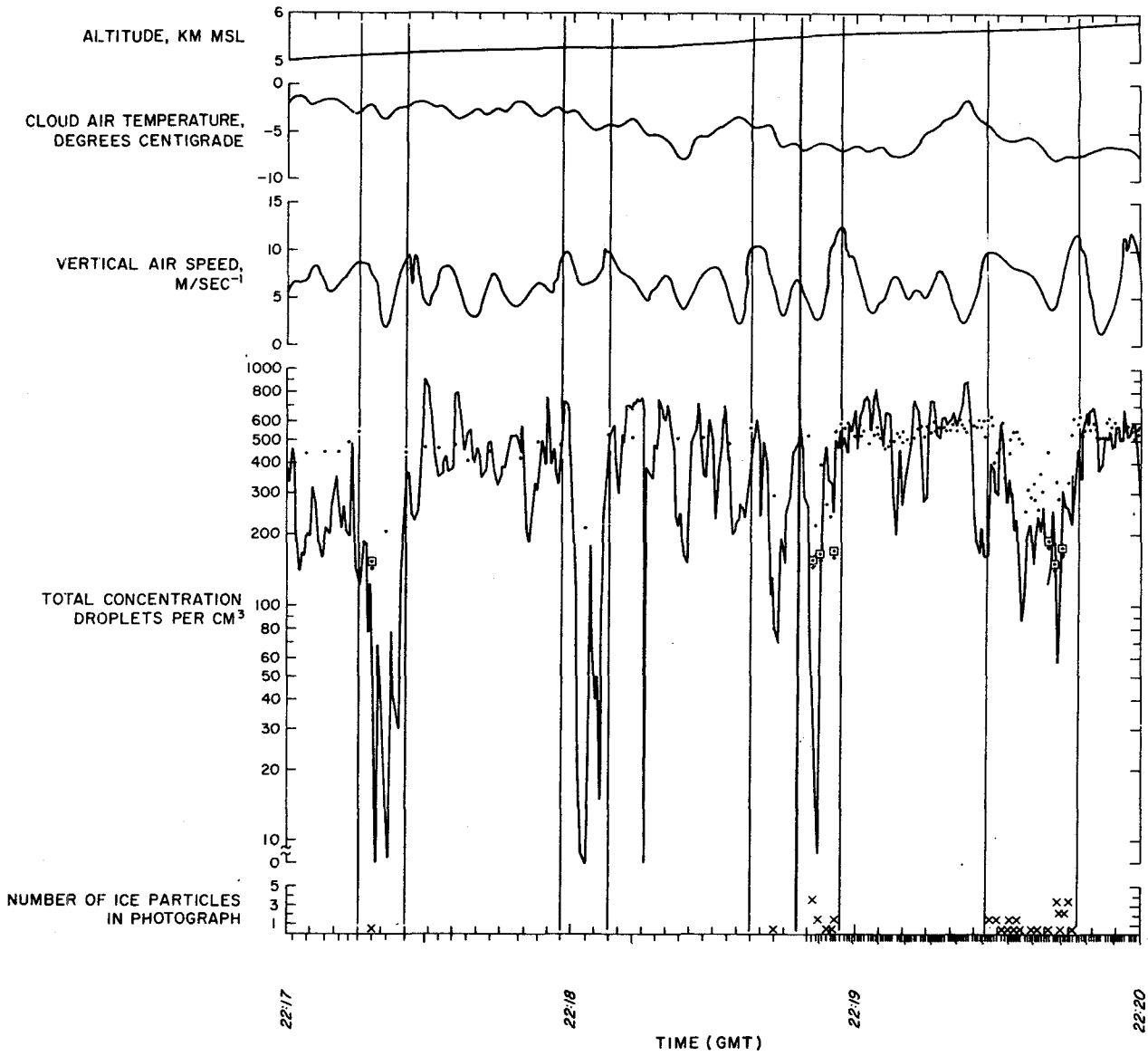

FIG. 4. Altitude, cloud air temperature, vertical airspeed, total droplet concentration and number of ice particles in photograph from 2217 GMT through 2220 GMT 15 June 1972. The solid line on the total droplet concentration plot represents data from the electrostatic disdrometer and the dots are data from the particle camera photographs using the overall fog level technique (see Cannon, 1974). Data points inside boxes with downward pointing arrows represent data from droplet concentrations below the linear portion of the film sensitivity curve and indicate concentration of an unknown amount below the approximately 150 cm^{-3} threshold. Vertical lines delineate bands of time where marked depletion of cloud droplets occurred frequently with the detection of ice particles by the particle camera photograph. Downward pointing marks at bottom of lower plot indicate time of a particle camera photograph. Photographs were taken at higher frame rate starting at 2218:50 when the occurrence of higher ice concentration was noted visually by the observer-camera operator.

typical of those encountered in the lower portion of the developing cumulus clouds in northeastern Colorado in the summertime when the temperature at cloud base is near 0°C. The vertical speed of the air is computed from the equation of motion of the sailplane using the variometer, airspeed and sailplane bank angle data. The liquid water content (g m^{-3}) is obtained by summing the cloud droplet distributions measured with the electrostatic cloud droplet probe. The presence or absence of ice particles is shown in the upper segment of the figure along with the vertical speed. The total droplet count per cubic centimeter taken from the particle camera photographs is indicated in the lower segment of the chart by a dotted line. The solid lines numbered 5, 6, 8, 9 and 11 refer to the characteristic radius of the cloud droplets in microns observed with the electrostatic disdrometer. The curve labeled T is total concentration per cubic centimeter obtained by summing the concentrations in all of the channels of the electrostatic disdrometer. The vertical scale for the

individual disdrometer channels is labeled on the left in number of droplets per cubic centimeter per micrometer interval of droplet radius. The vertical scale on the right gives the total number of cloud droplets observed in each 0.5 s sampling period (sample count) used to obtain the concentrations indicated on the left and therefore gives a measure of the statistical representativeness of the data.

The relationships between the air motion, total cloud droplet concentrations and the occurrence of precipitating ice particles is shown over a 3 min period in Fig. 4. Starting at the top, Fig. 4 plots show, respectively, the air temperature (°C), the vertical speed of the air (m s^{-1}), total droplet count (cm^{-3}) [connected line is for data from the electrostatic disdrometer and individual dots are for data from the camera] and the occurrence of the larger precipitating ice particles (x's show the total number of ice particles per camera frame).

In Fig. 4 the time spans where anomalously low droplet concentrations (delineated by vertical lines spanning the plot) were found were usually the same as those where ice particles were observed except for the second droplet depletion zone, where no ice particles showed in the single photograph taken during this period. The higher updraft speeds at the edges of the ice particle shaft with a diminished updraft in between are characteristic of the lower portion of the cloud. The sailplane's change in altitude (see top of Fig. 4) confirms the consistency of the updraft. Other sailplane flights in similar clouds show a change from an updraft to a downdraft when ice particles are encountered (Dye, 1975). These observations most probably demonstrate the effect of particle drag on the updraft and are due to the presence of the precipitating ice particles.

The sailplane spirals upward with a horizontal radius of ~300 m and an airspeed of ~40 m s^{-1}. Its vertical fall velocity with respect to the upward moving air varies with altitude and flight attitude, but on the average is roughly 1.5–2 m s^{-1}. The measurements illustrated in Fig. 4 were taken over a total flight path of 7.2 km and an altitude increase of 0.88 km. Thus, the variations in these data occur in both the horizontal and vertical with the greatest fluctuations appearing in the horizontal.

The coincidental appearance of ice particles (graupel) with diminished droplet concentrations seen in Fig. 4 is repeated at close to the time interval required for the sailplane to complete one 360° circuit (~42 s). This repeated coincidence suggests that the same precipitation shaft is being entered repeatedly at successively higher altitudes.

Fig. 5 is a reproduction of a particle camera photograph taken at 1619:22.5 MDT where the total droplet concentration in the in-focus volume is 800 cm^{-3}, the same as from the electrostatic disdrometer (see Figs. 3 and 4). No ice particles appeared nearby or at the time

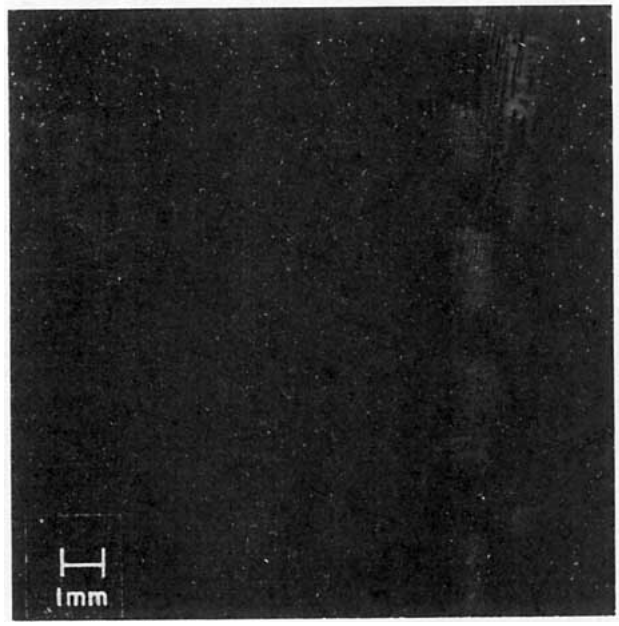

FIG. 5. Particle camera photograph taken at 2219:22.5 GMT 15 June 1972. Droplet concentration measured from the photograph and from the electrostatic disdrometer is 800 cm^{-3}.

the photograph in Fig. 5 was taken. The droplet concentrations show the effects of depletion in Fig. 6 which also shows an ice particle in the same volume at 1619:43. The droplet concentration in an equivalent in-focus volume measured from the photograph is 20 cm^{-3} and that measured by the disdrometer, 60 cm^{-3}. The observed depletion is confirmed in hundreds of similar

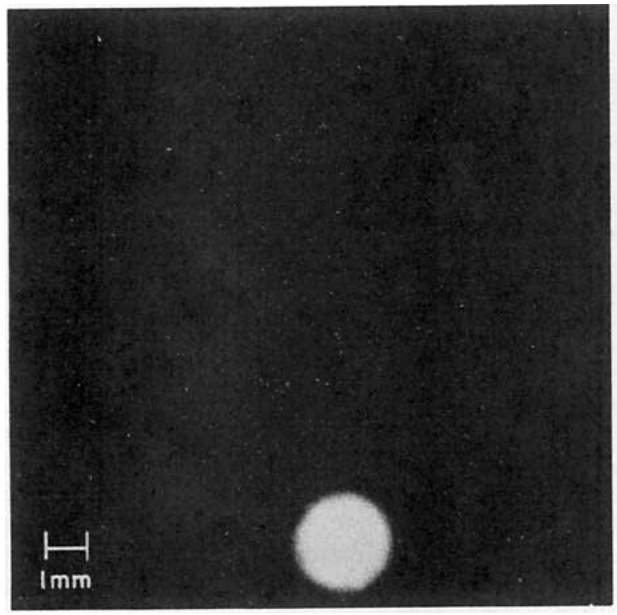

FIG. 6. As in Fig. 5 except at 2219:43 GMT. Droplet concentration measured from photograph is 20 cm^{-3} and concentration obtained by counting ice particle images is 5.3 ℓ^{-1}.

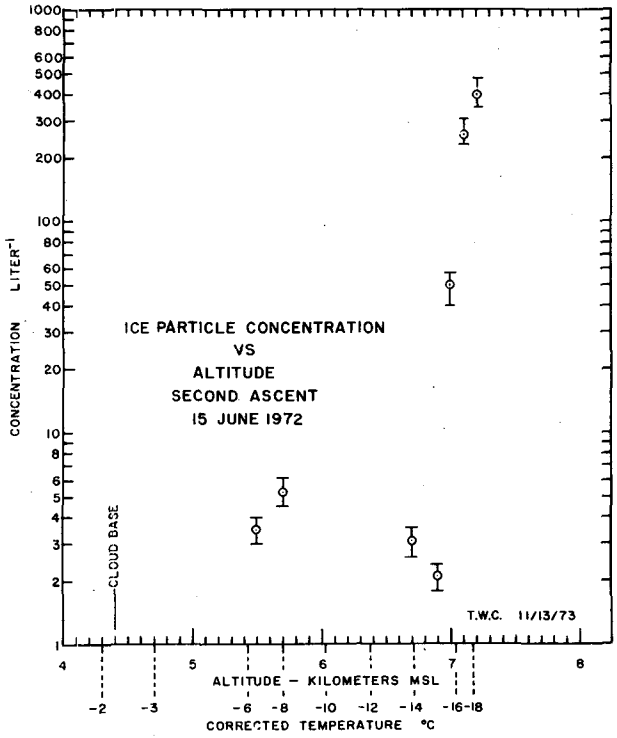

FIG. 7. Ice particle concentration vs altitude for cloud ascent on 15 June 1972. Length of vertical bars gives measurement error.

photographs and corresponding electrostatic disdrometer measurements. The particle camera typically photographs a 2.6 ± 0.5 cm^3 sample volume for 5 μm radius droplets, 5.2 ± 0.5 cm^3 for 10 μm, and 50 cm^3 for 0.5 mm radius droplets in each photograph (exposure time is 10 μs), while the electrostatic disdrometer samples a total volume of about 1 cm^3 of cloud cumulative over each 0.5 s interval. The cloud droplets in Fig. 6 have been largely depleted by accreting ice particles (graupel) in concentrations of 5.3 ℓ^{-1} like the image in the lower center portion of the photograph.

In this cloud the ice particle concentration (Fig. 7) increased by two orders of magnitude during an altitude ascent of less than 2 km in the updraft where the temperature decreased from -6 to -18°C. During the ascent the average diameter or long dimension of the ice particles decreased from approximately 2 mm to 0.2 mm (Fig. 8). The size range at each point is indicated in the figure by the thin vertical lines through the average size (open circles). The smaller ice particle sizes, size ranges and much higher concentrations in the upper portion suggest that this is where the newer ice particles are forming or collecting in the greatest numbers. The concentrations and sizes observed in the lower portion are more indicative of gravitational sorting, characteristics of the updraft profile and their past history rather than the cloud environment in which they are found. An attempt to sort out some of this apparent confusion will be discussed in the following sections.

4. Collating the observations

a. Discussion of collating process

Interpreting the observations in terms of where the ice particles formed and how they subsequently moved to arrive in the positions and concentrations observed is the primary task of collating the data obtained.

The flight path of the sailplane can be thought of as a helix in the surface of a circular cylinder which moves with the horizontal motion of the updraft, the axis of which will be distorted horizontally by the wind shear and tilted or deformed out of the vertical in the direction of the shear. Due to this flight pattern, the sailplane samples an updraft region where the most critical microphysical processes and convective motions occur. The data obtained are usually more directly related to the vertical path of the cloud droplets than is possible or practical with a larger aircraft making a number of horizontal traverses through a convective cell. In addition, the pilot flies to maximize his upward velocity, so that a quasi-Lagrangian sampling is obtained.

The measurements covered a sufficiently large portion of the cloud, and the air motions within it, that it became necessary for us to organize the data into a hypothetical quantitative framework in order to insure

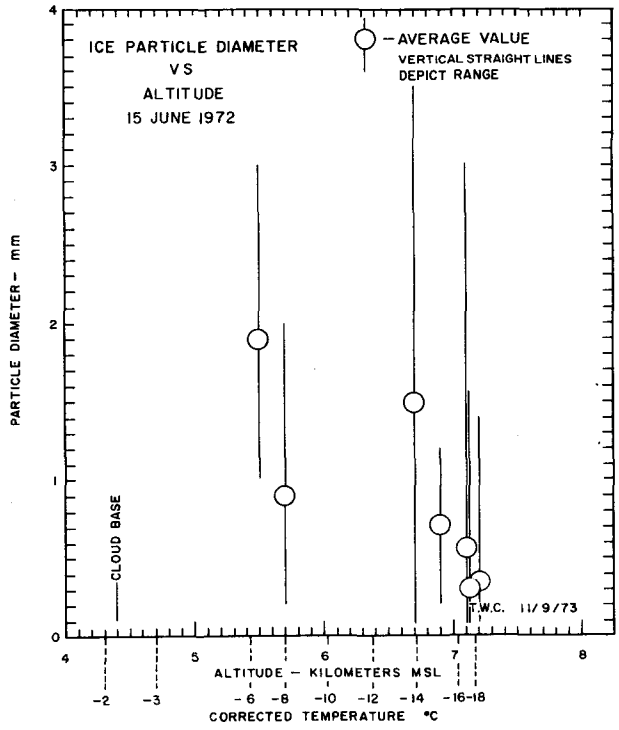

FIG. 8. Average long dimension of ice particle vs altitude for cloud ascent on 15 June 1972. Length of vertical bars gives total size range at each point.

that the sampled and unsampled regions of the cloud and its environment fit a compatible physical system. Hopefully, then, we could refer the particles observed at one altitude back to the region where they were formed, or at least explain the change in particle concentration, size and shape.

In order to accomplish this, we use a simulation of a simple convective cell circulation that obeys the equation of continuity and is parameterized to fit the observed updraft, cloud dimensions and environmental circulation. The atmospheric density in the cloud and its environment varies with height according to that of a standard atmosphere. Thermal characteristics and microphysical data within the cloud are taken from the sailplane observations. Local rawinsonde observations are used for the environmental wind and temperature. The circulation is therefore specified kinematically, while the consequences of this circulation on the trajectories of the cloud particles is calculated dynamically. The overall cloud dynamics and thermodynamics are not calculated but are assumed to be decoupled from the microphysics through the use of the sailplane observations of the air motions to specify the cloud circulation. We restrict the validity of our calculations to the effect of a single circulation cell on cloud particle distributions.

The sailplane can only gain altitude in a fairly consistent and organized updraft of 1.5–2 m s^{-1} or greater. This implies other organized horizontal air motions to sustain the updraft and somewhere in the atmosphere a downdraft or other compensating descending air.

The rapid repetition rate ($\leqslant 0.5$ s) observations of the combined cloud updraft and microphysics provide us with a large amount of data on the spatial distribution of cloud drop and ice particle spectra over extensive regions of actively growing and precipitating convective clouds. Even so, as we stated earlier, the origin and cause of the observed anomalies in the microphysical data are not clear from these observations alone. In particular, we wish to answer, as quantitatively as possible, the following questions:

- To what extent can the cloud air circulation of a single convection cell and gravitational sorting account for observed changes in size and concentrations of the precipitation particles in time and space?
- Is it possible for accretion to account for the observed precipitation shafts and the cloud droplet depletion within them?
- Can the observed precipitation growth rates and cloud water accumulation by the ice particles be accounted for by accretion?

b. Cell circulation synthesis

The circulation is formulated analytically from the type of convective cells that develop normally in a dynamic two-dimensional model of convection. To this convective circulation we add the environmental winds from the rawinsonde observations. The cell circulation is two-dimensional steady state and can be extended to three dimensions by assuming axial symmetry. The microphysics of the time-dependent precipitation growth is introduced into this circulation according to physical laws of the accretion process.

The analytical description of the convective cell circulation results from calculations of a two-dimensional dynamic simulation of convection typically produced by randomly distributed thermals near the surface (e.g., Drake *et al.*, 1975). The horizontal and vertical components of velocity in this circulation are

$$U_x(x,y)=C_1\left(\frac{x}{a}\right)\left[2\left(\frac{y+C}{a}\right)^2+\lambda a\left(\frac{y+C}{a}\right)-1\right]\times\exp\left[-\frac{1}{2}\left(\frac{x}{x_0}\right)^2-\left(\frac{y+C}{s}\right)^2\right]+U_{xe}(y), \quad (1a)$$

$$U_y(x,y)=C_1\left(\frac{y+C}{a}\right)\left[1-\left(\frac{x}{x_0}\right)^2\right]\times\exp\left[-\frac{1}{2}\left(\frac{x}{x_0}\right)^2-\left(\frac{y+C}{a}\right)^2\right]. \quad (1b)$$

Here $C=H_O-H_G$, where H_O the altitude of the maximum updraft and H_G the altitude of the ground, x_0 is the half-width of the updraft, $a=2^{\frac{1}{2}}C$, and $C_1=2^{\frac{1}{2}}U_y(0,0)/\exp(-\frac{1}{2})$, where $U_y(0,0)$ is the maximum updraft velocity. $U_{xe}(y)$ is the horizontal component of the environmental wind in the x direction as a function of height. A variety of observed profiles can be duplicated by adjusting the height of the maximum updraft, strength of the maximum updraft, the spacing $2x_0$ of the circulation poles, and the lower (H_G) boundary. This circulation is modified for the change in height of the density of the air, $\rho=\rho_0 e^{-\lambda y}$, where λ is the coefficient of y required to produce a standard atmosphere, ρ_0 being the air density at sea level. The horizontal translational wind velocity and the vertical shear of the horizontal wind can be added when required. Any nonzero wind shear will result in a circulation with a tilted updraft. The updrafts of multicell clouds may be simulated by superimposing the streamfunctions for any number of single cells to obtain the composite circulation.

All small cloud droplets (radius assumed $<20\,\mu$m normally) move with the air motion everywhere it has an upward component and disappear one timestep (usually 30 s) after the vertical component turns downward. Because of their small observed size they do not interact with each other. The variations with height of the liquid water content from the sailplane observations are fitted with a straight line approximation. The air density is the same inside and outside the "cloud" and

varies with height exponentially according to the Standard Atmosphere.

The embryonic precipitation particles are assumed to be spherical with an initial diameter of 100 μm. Growth of ice crystals to this size by vapor deposition in clouds containing many supercooled cloud droplets is very rapid, probably within the 30 s integration time-steps of the computer simulation. We have computed the trajectories and size distributions of the precipitation and hail growing from the accretion of supercooled cloud droplets by these ice particles. They are introduced at specified altitudes in concentrations appropriate to the temperature and nuclei concentration at that height in the cloud and

$$\frac{dm}{dt}=\pi r^2 EL|\mathbf{u}-\mathbf{v}|, \tag{2}$$

where dm/dt is the rate of mass increase of the ice particle, r the particle radius, E the collection efficiency, $\mathbf{u}$ the velocity of the air, $\mathbf{v}$ the particle velocity and L the liquid water content. As the mass and size of the ice particles increase, their terminal velocities change according to calculations based on empirical data (McDonald, 1960) for the drag coefficients of equivalent volume spheres and their motion computed according to a scheme used by Sartor (1970).

The effective streamfunction fields (denoted by the dashed lines in the illustrations) are the sum of the convective circulation vortex and the environmental vertically sheared horizontal wind in which the microphysical interactions are embedded. Other critical inputs are the cloud droplet and particle concentrations and sizes, the collection efficiencies, tilt of the updraft and cloud dimensions. A similar technique for relating tropical precipitation and cloud kinematics in one dimension is described by Kessler *et al.* (1963).

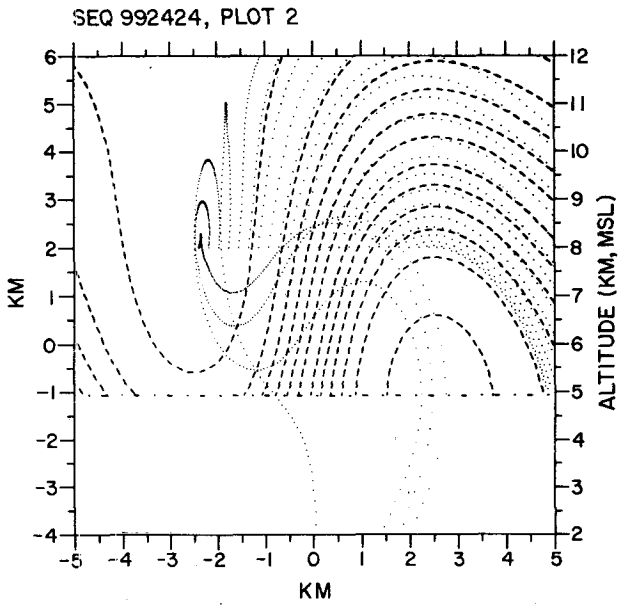

FIG. 9. Cloud simulation for 15 June 1972 case, ice particle initiation at 8.0 km. Streamlines are indicated as dashed lines, ice particle trajectories as dotted lines. Maximum updraft velocity is 10 m s^{-1} at 6 km, width of updraft 5 km, cloud base 4.9 km and cloud top 12 km; mean vector wind shear is 0.5 m s^{-1} km^{-1} and liquid water content $0.16y-0.72$, where y is altitude (km MSL).

c. Application of cell simulation to observations

1) 15 JUNE 1972

On 15 June 1972 the vector mean shear of the horizontal wind from the NHRE rawinsondes was found to be 0.5 m s^{-1} km^{-1} and the average upward motion obtained with the NOAA-NCAR cloud physics sailplane in the updraft of the developing cumulonimbus on this day was 10 m s^{-1} or greater.

Fig. 9 illustrates the computer output for 15 June 1972, the result of ice particle initiation at one altitude only, 8.0 km MSL.[2] The trajectories of the ice particles (dotted line) are depicted as they grow by the accretion of supercooled droplets. At each altitude where the ice particles are introduced, they are spread uniformly across the entire updraft. The trajectories in Fig. 9 starting in the first four positions from the left (west) form two precipitation shafts—one near the center of the updraft and one at the far right. The rapid ice particle growth occurs mostly as they cross the core of the updraft which supplies continuously a relatively undepleted supply of supercooled cloud droplets. In the precipitation shaft on the left side of the updraft in Fig. 9 one finds a bimodal distribution of the particle sizes as observed, due in this case to falling and rising precipitation particles in the same volumes of rising air. For ice particles initiated at 7.0 and 7.5 km a few small hailstones formed in crossing the updraft. At initiation altitudes of 6.5 and 8.0 km the graupel particles remained less than 5 mm diameter.

2) 23 JUNE 1972

On 23 June 1972 the vector mean shear of the horizontal wind from the rawinsondes was found to be 5 m s^{-1} km^{-1} and the average maximum upward motion obtained with the sailplane in the updraft of a developing cumulonimbus on this day was 20 m s^{-1} or greater. Cloud base was more than a kilometer lower, the cloud base temperature 12°C warmer, and the LWC at least four times as great as on 15 June. The streamlines of the circulation simulation for 23 June are shown in Fig. 10. The particle trajectories for ice particle calculations are for 6.5 km initiation altitude. Other runs made at 0.5 km intervals above 5.5 km are not depicted here. None of the trajectories beginning at 6.5 km and above results in hail or ice particles >5 mm diameter. This is in keeping with the sailplane pilot's report of clear and rime ice on the aircraft, but no visual or photographic observation of ice particles in the core of

[2] All altitudes are in km MSL.

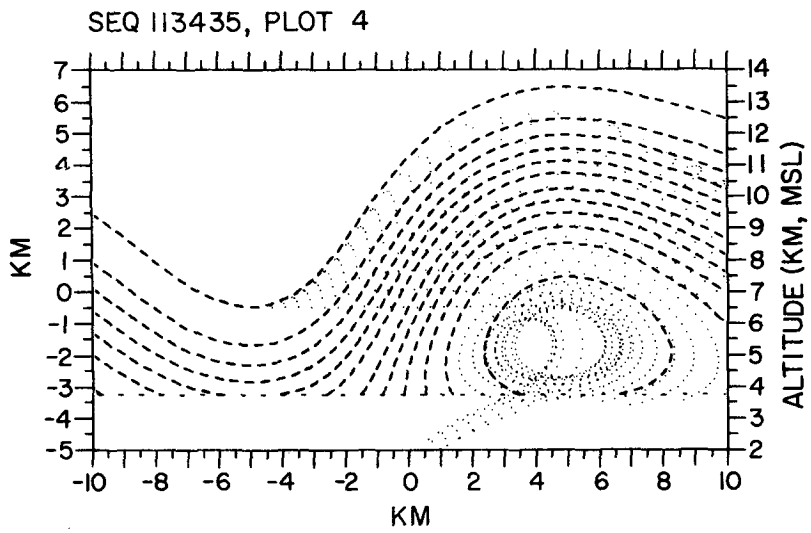

FIG. 10. Cloud simulation for 23 June 1972 with ice particle initiation at 6.0 km. Maximum updraft velocity is 20 m s^{-1} at 7 km, width of updraft 10 km, cloud base 3.7 km and cloud top 14 km; mean vector shear is 5 m s^{-1} km^{-1} and liquid water content $0.41y-0.96$, where y is altitude (km MSL).

the updraft. However, the camera was not operating much of the time in the uppermost portion of the cloud.

d. Cloud droplet depletion

Cloud droplet depletion is not simulated along with the other microphysics in keeping with observations over most of the cloud. In the limited regions of strong observed cloud droplet depletion and coexisting ice particles, we wish to determine if the observed localized depletion can be accounted for by the accretion of the supercooled cloud droplets by the observed ice particle distribution.

We assume that after the passage of each ice particle, the remaining cloud droplets instantaneously rearrange themselves so that in each sample unit volume they are always randomly distributed. Thus the number $N_i(\Delta t)$ of droplets remaining per unit volume after a small increment of time Δt is

$$N_i(\Delta t)=N_i(0)-\int_0^{\Delta t}\sum_j R_{ij}N_i(0)dt,$$

where $N_i(0)$ is the initial droplet spectrum and $R_{ij}=\pi E_{ij}N_j(r_j+r_i)^2(v_j-v_i)$, where the subscripts i and j refer, respectively, to the cloud droplets and the ice particles, E_{ij} is the collection probability, r_i and r_j are the equivalent radii of the particles and v_i and v_j their fall velocities. After the second Δt time interval,

$$N_i(2\Delta t)=N_i(\Delta t)-\int_0^{\Delta t}\sum_j R_{ij}N_i(\Delta t)dt.$$

Repeating this procedure K times gives

$$N_i(K\Delta t)=N_i(0)(1-\sum_m R_{ij}\Delta t)^K, \qquad (3)$$

which can be used to compute the number of droplets remaining in each droplet size interval i in a selected unit volume at $t=K\Delta t$, and the product $R_{ij}\Delta t$ is chosen so that it is less than 1.

Using Eq. (1) and the data taken from the sailplane flight of 15 June 1972 (Table 2) we compute the depletion of the observed concentrations of particles by calculating the fraction of the cloud droplets remaining after 1, 10, 20 and 60 s (Table 3). The density of the graupel particles (0.5 g cm^{-3}) given in Table 2 was estimated from their minimum fall velocity relative to the sailplane, and from the average graupel density observed by Jones (1960) and Heymsfield (1977, private communication). The fraction of the initial droplets remaining in each sample volume is very small after 1 min, showing that in a one-dimensional simulation or vertical updraft the graupel particles are capable of removing essentially all of the supercooled droplets within a precipitation shaft in accord with our observations. Outside the precipitation shafts, the cloud droplet population remains undepleted. In two or three dimensions where the updrafts can be tilted with respect to the falling particles a precipitation shaft is fed fresh supplies of cloud droplets from below and the effect of depletion on subsequent growth is minimized as assumed earlier.

5. Conclusions

Our conclusions are derived in some instances directly from observations and in others from our computational collations of the observed microphysics with a simple convective circulation cell of the observed developing cumulus clouds of northeastern Colorado on 15 and 23 June 1972. Despite the abundance of microphysical

TABLE 2. Typical cloud droplet and graupel particle distributions on 15 June 1972.

Cloud particles (number cm^{-3})		LWC [0.16Y*–0.72] (g m^{-3})	Assumed particle density (g cm^{-3})	Radius (cm)	LWC† or FWC†† (g m^{-3}) Σ drops / Σ graupel	Collection probability,** E_j $j=1$	$j=2$
Altitude 5.5 to 5.65 km MSL							
Droplets	i						
300	1		1.0	4.35×10^{-4}	0.103 LWC	0.5	0.85
40	2	[0.176] at 5.6 km	1.0	6.25×10^{-4}	0.041 LWC	0.6	0.90
				Total	0.144 LWC		
Graupel	j						
2.36×10^{-3}	1		0.5	0.060	1.070 FWC		
1.18×10^{-3}	2		0.5	0.135	6.080 FWC		
				Total	7.150 FWC		
Altitude 7.0 to 7.1 km MSL							
Droplets							
200	1		1.0	4.35×10^{-4}	0.0896 LWC	0.3	0.6
70	2		1.0	6.25×10^{-4}	0.0716 LWC	0.4	0.7
6	3	[0.408] at 7.05 km	1.0	7.75×10^{-4}	0.0117 LWC	0.8	0.9
				Total	0.1729 LWC		
Graupel	j						
392×10^{-3}	1		0.5	0.0150	2.78 FWC		
8×10^{-3}	2		0.5	0.0625	4.10 FWC		
				Total	6.88 FWC		

* Y =altitude (km MSL).
** See Sartor (1970).
† LWC =liquid water content.
†† FWC =frozen water content.

and air motion data, we are reporting only two contrasting meteorological situations. The multiplicity of hypotheses tested and their complexity do not particularly help this situation. The only mitigating circumstance that we can claim is that we have surveyed similar cases in 1971, 1972, 1973 and 1974 without finding serious contradictions with generalizations of the following specific conclusions:

1) The formation of precipitation shafts with bimodal size distributions in the middle and lower part of the cloud of 15 June 1972 can be recreated in a two-dimensional simulation of the observed cloud air circulation without the effect on the air motions of water loading or drag of the precipitation. Downdrafts will undoubtedly be created later on in the life history of natural clouds due to these forces, where initially an updraft existed.

2) The observed frozen water content (FWC) can increase by one to two orders of magnitude over the liquid water content (LWC) when moving from cloudy air into a precipitation shaft (see Table 2). A column of cloud air on 15 June 1972 at 5.5 km can be effectively depleted (98.5% complete, mostly with only the smallest sizes remaining) of supercooled cloud droplets by the observed distribution of ice particles in less than 60 s (Table 3). The FWC of the ice particles in a unit volume in the precipitation shafts at 5.5–7.1 km is an order of magnitude ($\sim$7 g m^{-3}) more water than the LWC of the supercooled cloud droplets in the same unit volume (0.22 g m^{-3}).

3) The change in concentration with height of the ice particles exceeds (by over two orders of magnitude) the expected ice nuclei concentration usually found in the atmosphere at comparable temperatures. As shown

TABLE 3. Fraction F_{ij} of supercooled droplets remaining after passage of graupel in a selected unit volume. Particle distributions from Table 2.

	Time(s) 1	10	20	60
Altitude 5.5–5.65 km MSL				
Fraction remaining	0.928	0.473	0.223	0.0155
Fall distance of (0.6 mm radius) graupel	5.88 m	58.8 m	117.6 m	352.8 m
Fall distance of (1.35 mm radius) graupel	11.0 m	110.0 m	220.0 m	660.0 m
Altitude 7.0–7.1 km MSL				
Fraction remaining	0.951	0.609	0.373	0.0544
Fall distance of (0.15 mm radius) graupel	1.42 m	14.2 m	28.4 m	85.2 m
Fall distance of (0.625 mm radius) graupel	6.33 m	63.3 m	126.6 m	379.8 m

numerically, the organized cloud air circulation cell required to produce the observed updraft can account for some fraction of this increase through the three-dimensional convergence of the ice particles; this offers at least partially an alternative to ice particle multiplication as an explanation for a deficiency of ice nuclei compared to observed ice particle concentrations. In the case of the 15 June 1972 observations the simulations indicate this effect is a little over one order of magnitude of the two orders of magnitude increase from 5.5 to 7.1 km.

4) The average concentrations of ice particles observed on 15 June 1972 exceed 400 ℓ^{-1} over a substantial region near the top of the sailplane flight in this cloud. Concentrations exceeding 100 ℓ^{-1} have been observed on numerous occasions on other days and sometimes in other areas. This is two orders greater than the concentration targeted for on the NHRE seeded days.

5) The cloud penetrated on 23 June 1972 showed higher temperatures, moister air and stronger instability and therefore more rapid coalescence than that of 15 June 1972, where the appearance of larger numbers of ice accreted particles occurred before coalescence could effectively start.

6) The use in these calculations of a two-dimensional cell circulation for simulations of simple cloud processes seems to have been useful for reproducing anomalies in the observed precipitation particle size and concentration as well as their distribution in space in the cloud and as fallout or blowoff from the cloud. The assumption of continuous microphysical growth of precipitation, as suggested by the observations, does not seem to have adversely affected the results. It is probable that the less detailed microphysics and the substitution of observations of cloud parameters in place of more sophisticated one-dimensional stochastic microphysics and thermodynamic calculations are offset by the use of two dimensions.

We are speaking in this case of quantitative calculations of the gross cloud properties and not of detailed quantitative modeling.

Acknowledgments. The authors wish to thank Dr. Vim Toutenhoofd for his skillful piloting of the *Explorer;* Dr. James E. Dye for his supervision of the sailplane project; Mrs. Dorene Howard for typing this manuscript; Mr. Larry McElhaney for help with the artwork and processing of camera photographs; and Ms. Hing L. Ng and Ms. Lynn Udick for assistance with the photographic printing and computer runs.

REFERENCES

Abbott, C. E., J. E. Dye and J. D. Sartor, 1972: An electrostatic cloud droplet probe. *J. Appl. Meteor.*, **11**, 1092–1100.

Cannon, T. W., 1974: A camera for photography of atmospheric particles from aircraft. *Rev. Sci. Instr.*, **45**, 1448–1455.

Drake, R. L., P. D. Cagle and D. P. Anderson, 1975: Interactive line thermals in a convective layer: A numerical simulation. *J. Atmos. Sci.*, **32**, 302–319.

Dye, J. E., 1975: A case study of microphysical development in new cells of a multicell storm. *Preprints NHRE Symposium/Workshop on Hail*, NCAR, Pap. VII.C2.

Jones, R. F., 1960: Size distributions of ice crystals in cumulonimbus clouds. *Quart. J. Roy. Meteor. Soc.*, **86**, 187–194.

Kessler, E., E. A. Newburg, P. J. Feteris and G. Wickham, 1963: Relationships between tropical precipitation and kinematic cloud models. Rep. 4, Contract DA 36-039 SC 89099, DA Project 3A 99-27-005, The Travelers Research Center, Inc., Hartford, Conn., 52 pp.

Knight, C. A., N. C. Knight, J. E. Dye and V. Toutenhoofd, 1974: The mechanism of precipitation formation in northeastern Colorado cumulus. I. Observations of the precipitation itself. *J. Atmos. Sci.*, **31**, 2142–2147.

McDonald, J. E., 1960: An aid to computations of terminal fall velocities of spheres. *J. Meteor.*, **17**, 463–465.

Sartor, J. D., 1970: Accretion rates of cloud drops, raindrops, and small hail in mature thunderstorms. *J. Geophys. Res.*, **75**, 7547–7558.

——, 1972: Clouds and precipitation. *Physics Today*, **25**, 32–38.

——, and V. Toutenhoofd, 1973: The Explorer—The sailplane as an atmospheric probe. *Atmos. Tech.*, **1**, 34–36.

Todd, C. J., 1965: Ice crystal development in a seeded cumulus cloud. *J. Atmos. Sci.*, **22**, 70–78.